

Selection and Characterization of Anti-MUC-1 scFvs Intended for Targeted Therapy¹

Michelle D. Winthrop, Sally J. DeNardo,²
Huguette Albrecht, Gary R. Mirick,
Linda A. Kroger, Kathleen R. Lamborn,
Česlovas Venclovas, Michael E. Colvin,
Patricia A. Burke, and Gerald L. DeNardo

University of California Davis Medical Center, Sacramento, California 95816 [M. D. R., S. J. D., H. A., G. R. M., L. A. K., P. A. B., G. L. D.]; University of California San Francisco, San Francisco, California 94143 [K. R. L.]; Lawrence Livermore National Laboratory, Livermore, California 94550 [Č. V., M. E. C.]; and Institute of Biotechnology, 2028 Vilnius, Lithuania [Č. V.]

Abstract

Purpose: The selection and characterization of anti-MUC-1 single-chain antibody fragments (scFv) is a first step toward the construction of new anticancer molecules designed for optimal blood clearance and tumor penetration. The mucin MUC-1 was chosen as an antigen because it is abundantly expressed on epithelial cancers in an aberrantly glycosylated form, making it structurally and antigenically distinct from MUC-1 expressed on normal cells.

Experimental Design: A previously constructed anti-MUC-1 phage display library from hyperimmunized mice, with 5×10^5 calculated variants, was screened for the selection of anti-MUC-1 scFvs. Selection criteria were high binding to a MUC-1 peptide containing 4 tandem repeats of 20 amino acids and to MUC-1-positive MCF-7 (human breast cancer) cell lysates in ELISA.

Results: Six anti-MUC-1 scFv clones were selected and characterized. Nucleotide sequencing showed that four of them were full length scFv genes (variable heavy chain + variable light chain), whereas the remaining two contained either a variable heavy chain or a variable light chain alone. Their binding affinities (K_a) range between 8×10^7 and 10^9 M⁻¹. Immunohistopathology demonstrated reactivity with breast cancer cells (MCF-7 and BT20) and human breast biopsy tissue. Molecular modeling revealed high structural similarity of the anti-MUC-1 scFvs with the X-ray-determined structure of the anti-CEA scFv (MFE-23).

Conclusions: *In vitro* antigen binding was demonstrated for the selected anti-MUC-1 scFvs. The binding affinities of these scFvs are in a promising range for efficient *in vivo* antigen binding. These anti-MUC-1 scFvs will be evaluated as antigen-binding modules in new multifunctional agents for the detection and therapy of cancer.

Introduction

Although radioimmunotherapy using intact MAbs³ has been studied in clinical trials for the treatment of breast cancer and other solid tumors, therapeutic success has been limited by the large size of the MAb (150 kDa) molecules which retards blood clearance and decreases the accumulation of the radio-pharmaceutical in the tumor (1). Recombinant antibodies and their fragments in combination with new therapy approaches such as pretargeting have become a promising resource for the design of high-affinity specific targeting drugs (2, 3). Recent construction of engineered targeting molecules has demonstrated the potential for multivalent high affinity reagents built from small binding fragments (25 kDa), which can potentially target tumor more efficiently than large MAbs (4). Antibody fragment units have also been engineered for gene therapy, imaging, immunotherapy, radioimmunotherapy, chemotherapy, and prodrug therapy (5–13). ScFvs³ corresponding to the VH³ and VL³ immunoglobulin domains connected by a biologically inert flexible linker create the smallest antibody fragments that usually retain specific binding characteristics. ScFv molecules can be produced from existing MAb hybridoma clones, however, phage display libraries can provide a multitude of scFvs from a more diverse antibody gene pool and thus allow for the selection of scFvs to various epitopes and with a range of binding characteristics (14–19).

One of the epithelial mucin family of molecules, MUC-1, has received considerable interest as a cancer antigen target. It is abundantly expressed on a number of epithelial cancers, where its aberrant distribution and glycosylation make it structurally and antigenically distinct from MUC-1 expressed by nonmalignant cells (20–23). The dominant form of MUC-1 is a high molecular weight molecule, comprised of an extracellular mucin domain with tandem repeats of 20 amino acids, a trans-membrane region, and a cytoplasmic tail. Within the extracellular domain, novel epitopes of shortened carbohydrate chains and portions of the 20 amino acid tandem repeats are exposed in malignant cells and hence provide specific targets for antibodies (24–26). In normal epithelial tissue, MUC-1 is localized to the

¹ Presented at the “Ninth Conference on Cancer Therapy with Antibodies and Immunoconjugates,” October 24–26, 2002, Princeton, NJ. This work was supported by U.S. Department of Energy Grant DE-FG01-00NE22944, California Breast Cancer Research Program Postdoctoral Fellowship Grant [M. D. W.], a Society of Nuclear Medicine Education and Research Foundation Fellowship [M. D. W.], and National Cancer Institute Grant CA-47829.

² To whom requests for reprints should be addressed, at Radiodiagnosis and Therapy, Molecular Cancer Institute, University of California, Davis Medical Center, 1508 Alhambra Boulevard, Room 3100, Sacramento, CA 95816. Phone: 916-734-3787; Fax: 916-451-2857; E-mail: sjdenardo@ucdavis.edu.

³ The abbreviations used are: MAb, monoclonal antibody; K_a , binding affinity; PDB, Protein Data Bank; scFv, single-chain antibody fragment; VH, variable heavy chain; VL, variable light chain; ITPG, isopropyl- β -D-thiogalactopyranoside; TES, 0.2 M Tris-HCl (pH 8.0), 0.5 mM EDTA, 0.5 M sucrose.

apical region of the cells, but in malignant tissue, MUC-1 expression is up-regulated, and its distribution is no longer confined to the apical region (27). MUC-1 has been demonstrated to play a role in cell adhesion, cell signaling, and immune responses (24–26, 28). Consequently, overexpression of MUC-1 resulting in decreased cell adhesion may be associated with tumor metastasis (23, 29). A substantial number of anti-MUC-1 MAbs have been produced against this glycoprotein, with the majority of them recognizing epitopes within the tandem repeat region (20–22, 30–33). These anti-MUC-1 MAbs have been used primarily as *in vitro* diagnostic agents to identify tumor markers and monitor levels of circulating antigen (34). A few have been used to deliver radiation to advanced tumors as in radioimmunotherapy (35). In ovarian cancer, the anti-MUC-1 HMFG1 antibody has been used to deliver ^{90}Y to peritoneal implants in patients with minimal residual disease (36, 37). Another MUC-1 MAb (BrE-3) labeled with ^{90}Y has been used in the treatment of breast cancer; transient and partial tumor responses were seen in a population of patients who had been heavily pretreated with other cancer therapeutics (36, 38–41). These studies confirm that this tumor antigen can be effectively targeted without also targeting MUC-1 in normal tissue (36, 37).

Here, we describe the selection of anti-MUC-1 scFvs from a previously constructed hyperimmunized mouse anti-MUC-1 phage library (42). Six anti-MUC-1 scFvs were chosen for further characterization because of their consistent reactivity to the MCF-7 human breast cancer cell line. The characteristics of these scFvs will be useful in the selection of ideal agents for imaging and as pretargeting and therapy agents.

Materials and Methods

Culture of Human Cell Lines. MUC-1-positive human breast adenocarcinoma cell line MCF-7 cells (American Type Culture Collection, Manassas, VA) were grown to 75% confluence in DMEM (Life Technologies, Inc., Invitrogen Corp., Carlsbad, CA) medium containing 5% FCS. BT20 breast cancer cells (American Type Culture Collection) were grown in MEM with Earle's salts (Life Technologies, Inc., Invitrogen Corp.) containing nonessential amino acids (0.1 mM) and 10% FCS.

Library Construction and scFv Selection. These procedures have been described previously (42). Briefly, BALB/c mice (Harlan Sprague Dawley, Indianapolis, IN) received an i.p. injection of MUC-1-positive MCF-7/HBT 3477 (10:1) cell membrane lysate, followed by three immunizations with keyhole limpet hemocyanin-MUC-1 synthetic peptide at 3-week intervals. The 80 amino acid MUC-1 peptide corresponds to 4 repeats of the 20 amino acid sequence from the extracellular tandem repeat domain of MUC-1. The amino acid sequence of one repeat is: PDTRPAGSTAPPAHGVTS (43). The scFv library was constructed using the RPAS mouse scFv module (Amersham Biosciences Corp., Piscataway, NJ). For affinity selection, the phages were subjected to three rounds of affinity selection in a 3% nonfat milk/PBS buffer (pH 7.4; Sigma-Aldrich, St. Louis, MO) solution containing 0.2% Tween 20 with decreasing amounts (100, 50, and 10 nM) of MUC-1 peptide conjugated to biotinylated BSA and magnetic streptavidin beads (Dynal, Inc., Lake Success, NY). Selected phages

were amplified by reinfection of *Escherichia coli* TG1 cells, before the next selection round.

ScFv DNA Sequence Analysis. The anti-MUC-1 plasmids were extracted from TG1 *E. coli* using the Qiafilter plasmid extraction kit and protocol (Qiagen, Valencia, CA). Both DNA strands of the anti-MUC-1 scFvs were sequenced (DBS automated DNA sequencing facility, University of California at Davis, Davis, CA).

ScFv Production. ScFv clones for ELISA testing were grown overnight in cell culture plates at 30°C with shaking at 200 rpm in 2xYT media (17 g/liter Bacto-tryptone, 10 g/liter Bacto-yeast extract, 5 g/liter NaCl) containing 2.0% glucose and 100 µg/ml ampicillin. The following day, after changing the medium to 2xYT + ampicillin, scFv expression was induced overnight at 30°C by addition of IPTG³ (USB, Cleveland, OH) to 1 mM final concentration (44). Larger scale production of soluble anti-MUC-1 scFv protein for Scatchard and immunohistochemistry analyses was conducted in shaker flasks or in a 5 liter Bioflo 3000 fermentor (New Brunswick Scientific Co., Inc. Edison, NJ). For culture in flasks, *E. coli* containing the scFv gene was inoculated into 2xYT medium containing 2% glucose and 100 µg/ml ampicillin. The culture was grown for 8 h at 30°C, then diluted 1:1000 using 2xYT medium containing 2% glucose and 100 µg/ml ampicillin, and grown for an additional 16 h. The bacteria were pelleted by centrifugation at 6300 × *g* for 15 min at 4°C using a Sorval centrifuge with a GSA rotor and resuspended in 2xYT medium containing 1 mM IPTG and 100 µg/ml ampicillin for soluble scFv protein production at 30°C for 4.5 h. Culture in the biofermentor was conducted as described previously (45), with the following changes: ampicillin was used as the selective agent; and the scFv protein expression was induced by addition of IPTG to a final concentration of 1 mM.

ScFv Purification. ScFvs were purified as soluble proteins from the periplasm of the *E. coli* bacteria by pelleting 1 liter of culture and resuspending the bacteria in 20 ml of TES.³ This was followed by the addition of 33 ml of 0.2× TES and incubation for 30 min on ice with moderate agitation. The cell debris were pelleted by centrifugation at 12,000 × *g* for 30 min at 4°C. The anti-MUC-1 scFv proteins were purified from the filtered (0.45 µm) supernatant by affinity column chromatography using the RPAS purification module (Amersham Biosciences Corp.). The purified scFvs were stored in PBS, pH 7.4.

ELISA Selection. MCF-7 cell lysate was used to further select MUC-1 binding scFv clones. MCF-7 lysates containing membrane fragments were prepared according to a previously described protocol (46). The total protein content of the cell lysates was determined using the Micro BCA protein assay reagent kit (Pierce Chemical Co., Rockford, IL). Pro-Bind ELISA assay plates (Becton Dickinson Labware, Franklin Lakes, NJ) were coated overnight at room temperature with MCF-7 cell lysate (200 µg/well) in 15 mM sodium bicarbonate buffer, pH 9.6. The ELISA plates were rinsed with PBS and blocked with PBS containing 3.0% dried nonfat milk for 1 h at room temperature. Tween 20 (10 µl/well) was added to the Pro-Bind plates followed by the addition of the anti-MUC-1 scFv protein (90 µl/well). BSA, 10% in PBS, was used as a negative control. Incubations were conducted at 37°C for 1 h. After each incubation, the plates were washed three times with

PBS containing 0.05% Tween 20 followed by three washes with PBS only. The bound scFvs were detected with 100 μ l of anti-E-Tag-horseradish peroxidase MAb (1:250) (Amersham Biosciences Corp.) in 3% nonfat milk solution. After the last washing step, the 2,2'-aminobis-3-ethylbenzthiazoline-6-sulfonic acid substrate (Sigma-Aldrich), containing 0.3% H₂O₂ was added. As soon as the colorimetric reaction had developed, the plate was read at A₄₀₅ (Dynex microplate reader, Chantilly, VA).

Affinity Evaluation by Competitive ELISA. Competitive ELISA analyses were performed in plates coated with MCF-7 cell lysate. Pro-Bind ELISA assay plates were coated overnight at room temperature with the MCF-7 cell lysate (200 μ g/well) in 15 mM sodium bicarbonate buffer, pH 9.6. Subsequently, the ELISA plates were rinsed with PBS and blocked with PBS containing 3.0% dried nonfat milk for 1 h at room temperature. Soluble scFv was diluted in 10% Tween 20 and stored on ice until used. MUC-1 peptide used as the competitor was diluted in 3% nonfat milk to provide the following concentrations of 0, 1, and 10 nM. BSA, 10% in PBS, was used as a negative control. After 30 min of incubation at room temperature, the soluble scFvs with or without various concentrations of the competitor were transferred to ELISA plates. Incubations were carried out at 37°C for 1.5 h. After each incubation, the plates were washed three times with PBS containing 0.05% Tween 20 followed by three washes with PBS only. Anti-E-Tag-horseradish peroxidase MAb, 100 μ l (1:250) in 3% nonfat milk, was added to the wells, and the plate was incubated. The plate was developed by addition of the 2,2'-aminobis-3-ethylbenzthiazoline-6-sulfonic acid substrate containing 0.3% H₂O₂ before reading at A₄₀₅.

ScFv K_{as}^3 were extrapolated from the competitive ELISA data based on linear regression and covariance analyses. Linear regression was used to estimate the binding affinities using all of the data points determined from three individual experiments in which each specific concentration was performed in triplicate, whereas analysis of covariance was used to calculate the variability of the affinity estimates of the scFv by grouping the data into individual trials.

Scatchard Analysis. One anti-MUC-1 scFv (12E) was iodinated by chloramine T as described previously (47). The specific activity of the product was 0.46 mCi/mg. High performance liquid chromatography was used to purify the ¹²⁵I-12E scFv by applying 200 μ l of the ¹²⁵I-12E scFv onto a SEC-2000 column (Phenomenex, Torrance, CA) and collecting 0.5 ml fractions. ¹²⁵I-12E scFv fractions corresponding to 42 kDa (dimeric form) and 25 kDa (monomeric form) were collected and used in competitive binding assays. Unlabeled 12E scFv was purified into 42 kDa and 25 kDa fractions as described above for use as competitor to labeled ¹²⁵I-12E scFv. ¹²⁵I-12E scFv (0.1 μ g) was added to 5% BSA-PBS solution along with various amounts of unlabeled immun conjugate (0.5, 1.0, 2.0, and 5.0 μ g). MCF-7 cells (5.0×10^5) were added, and the final volume was adjusted to 150 μ l. The solutions were gently vortexed and incubated at room temperature for 1 h. After the cells were pelleted by centrifugation, the supernatant was carefully removed and transferred to a clean vial. Supernatants and pellets were counted using a LKB 1282 Compugamma CS well counter (Amersham Biosciences Corp.). Scatchard analysis

from a competitive binding assay using MCF-7 cells was used to estimate the binding affinities of the dimeric and monomeric 12E scFvs.

Molecular Modeling. Database searches showed several scFv constructs, with experimentally determined three-dimensional structures, to be similar to the 12E scFv. From these, the structure of the murine scFv antibody MFE-23 (PDB³ code: 1QOK) was selected as a template because it had the closest sequence homology (73% identical residues) as well as an identical linker sequence connecting the VH and VL domains (48). Conformation for the conserved structural regions of clone 12E was assigned directly from the structural template. The six hypervariable loops (H1 to H3 and L1 to L3), responsible for antigen binding, were modeled using additional structural information from the PDB, as follows. First, the PDB was searched for loop structures that had high sequence similarity to these six loop regions in the 12E scFv. Four of the hypervariable loops (H2, L1 to L3) had similar conformations in both the original template (MFE-23) and the set of structures with the closest sequence similarity to the 12E protein. The structures of two of the loops (H1 and H3) in MFE-23 were different from the consensus structure observed by comparing corresponding loops that were the most similar by sequence to the 12E scFv. Therefore, H1 and H3 loops of 12E scFv were modeled using the consensus loop structures and not the H1 and H3 loops from the MFE-23 scFv.

The structure of the VH domain for the 3D scFv was obtained using the same procedure applied to clone 12E. Estimation of secondary structure for the 3D scFv COOH-terminal region was done using PsiPred (49). Model-building was performed using MODELLER (50), followed by model quality assessment with Procheck (8).

Immunohistochemistry. Cytospin preparations of MUC-1-positive MCF-7 cells and BT20 breast cancer cells were used to compare immunohistochemical staining by purified anti-MUC-1 scFv and control nonbinding scFv to staining by anti-MUC-1 MAb BrE-3 (gift from R. L. Ceriani) and control IgG1 MAb (R&D Systems, Minneapolis, MN), respectively. The murine MAb BrE-3 reacts with an epitope on the tandem repeat of the peptide core of MUC-1 (51). It has also been shown to react with >75% of the cells in >95% of the breast cancers (52). The negative control scFv, corresponding to an antilymphoma scFv (53), was produced and purified in the same manner as anti-MUC-1 scFvs described above. Freshly scraped cells were resuspended in PBS, spun onto superfrost plus slides (Thermo Shandon, Pittsburgh, PA), and fixed in 10% formalin for 10 min. After a washing in PBS, the slides were incubated with 0.3% H₂O₂ in methanol for 10 min, followed by PBS wash. The cells were blocked with 10% goat serum in PBS for 10 min, followed by incubation with MAb (BrE-3 and control IgG1, 5 μ g/ml) or scFv (control and 12E, 26 μ g/ml) overnight at 4°C in a humidified chamber. After rinsing in PBS, the slides were incubated with biotinylated antimouse MAb (Molecular Probes, Eugene, OR) for 1 h, rinsed, and incubated with ABC reagent (Vector Laboratories, Burlingame, CA). Color development was performed using 3,3'-diaminobenzidine tetrahydrochloride (Vector), followed by counterstaining with Mayer's modified hematoxylin (Master Tech, Lodi, CA). Breast tissue fixed in formalin and embedded in paraffin was cut into 5- μ m sections

A VH

```

12E QVKLQSGTEVVKPGASVKLSCKASGYIFTSYDIDWVRQTPEQGLEWIGWIFPGEGETEY 60
3D QVKLQSGTEVVKPGASVKLSCKASGYIFTSYDIDWVRQTPEQGLEWIGWIFPGEGETEY 60
C4 QVKLQSGTEVVKPGASVKLSCKASGYIFTSYDIDWVRQTPEQGLEWIGWIFPGEGETEY 59
E2 QVKLQSGTEVVKPGASVKLSCKASGYIFTSYDIDWVRQTPEQGLEWIGWIFPGEGETEY 59
A5 QVKLQSGTEVVKPGASVKLSCKASGYIFTSYDIDWVRQTPEQGLEWIGWIFPGEGETEY 57
2B QVKLQSGTEVVKPGASVKLSCKASGYIFTSYDIDWVRQTPEQGLEWIGWIFPGEGETEY 57

12E NEKFKGRATLSVDRKSSSTAYMELTRLTSEDSAVYFCARGDYRRYFDLWGGQTTVTVS 118
3D NEKFKGRATLSVDRKSSSTAYMELTRLTSEDSAVYFCARGDYRRYFDLWGGQTTVTVS 118
C4 NEAFISRLNINKDNRKSGVFFKVDLSLQDDRGIIYCVRR--RNGYFFDSWGQTTVTVS 115
E2 NEAFISRLNINKDNRKSGVFFKVDLSLQDDRGIIYCVRR--RNGYFFDSWGQTTVTVS 114
A5 IQLSYPDTSTR--TTPRAKFLKWTYVNLMTREAYTTVGV--MGTSLTPGANGTTVTVS 111
2B IQLSYPDTSTR--TTPRAKFLKWTYVNLMTREAYTTVGV--MGTSLTPGANGTTVTVS 111

```

B VL

```

12E DIELTQSPAIMSASPGERVMTCSASSSIRY----IYWYQQKPGSSPRLLIYDTSNVA 55
3D DIELTQSPGVKTI-----IYWYQQKPGSSPRLLIYDTSNVA 52
C4 DIELTQSPASLLCLWGRGPPSHAGPTMVTSTSGYNYIYWSQQKPGSSPKLLIYLSNLES 60
E2 DIVLTQSPASLLIYLGWRGPPSHAGPTMVTSTSGYNYIYWSQQKPGSSPKLLIYLSNLES 60
A5 DISSLSLQLP-LYLWGRGPPSHAGPTMVTSTSGYNYIYWSQQKPGSSPKLLIYLSNLES 58
2B ----TQSPLELLIYLGWRGPPSHAGPTMVTSTSGYNYIYWSQQKPGSSPKLLIYLSNLES 56

12E GVFFRSGSGSGTSYSLTINRMEADAA--TYCQEWNSGYPTTGGGTKLELKRAAA 110
3D -----CTKLELKRAAA 23
C4 GVEARVSGSGSHTYFTLNHPVEEEDAAATFYCRHTRLEPCTFGGRTKLEIKRAAA 116
E2 GPCQVQWVWDRLHPQHSCGGRCCLQPTVSTLGAY--TFGGGTKLELKRAAA 113
A5 GPCQVQWVWDRLHPQHSCGGRCCLQPTVSTLGAY--TFGGGTKLELKRAAA 111
2B GPCQVQWVWDRLHPQHSCGGRCCLQPTVSTLGAY--TFGGGTKLELKRAAA 110

```

Fig. 1 Sequence analyses. Amino acid sequences of the VH (A) and VL (B) antigen binding regions of the anti-MUC-1 12E, 3D, C4, A5, E2, and 2B scFvs are provided. The 3D scFv (VH only) appears to be a truncated version of the 12E scFv.

onto Super Frost Plus slides. After deparaffinization and rehydration, tissues were treated similarly to cells, with the addition of microwave antigen retrieval (3×5 min at 600 W in 10 mM sodium citrate, pH 6). Cells and tissues were photographed at $\times 400$ magnification.

Results

ELISA Selection. Six scFv clones were selected from ELISA results, indicating that they consistently bound MUC-1 peptide and membrane lysate of the MCF-7 breast adenocarcinoma cells.

DNA Sequence Analysis. Automated DNA sequencing established that four of the six scFvs contained both the VH and VL sequences that form the antigen binding site. The remaining two scFvs contained either the VL sequence (2B) or the VH sequence (3D) alone (Fig. 1). The 12E and 3D scFvs have identical VH sequences. Despite the lack of a VL domain, the 3D scFv was intensely reactive with MCF-7 cell lysate in ELISA.

Competitive ELISA. Four of the six initially selected anti-MUC-1 scFvs were chosen, because of their consistent binding to MCF-7 cell lysate, to be tested in this assay. Preincubation of these scFvs with increasing amounts of MUC-1 competitor peptide interfered with their binding to the plated MCF-7 cell lysate (Fig. 2). In the presence of 1 nM competitor, three of the four scFvs tested were partially inhibited from subsequent binding to the plated MCF-7 cell lysate. The inhibition percents were 52% for the C4 scFv, 19% for the 3D scFv, and 44% for the 12E scFv. A 10-fold increase in the amount of competitor (10 nM) resulted in estimates of binding inhibition of 66% for the C4 scFv, 68% for the 3D scFv, 45% for the 12E scFv, and 13% for the A5 scFv.

These competitive ELISA data, from three separate experiments performed in triplicate, were used to extrapolate the K_a s

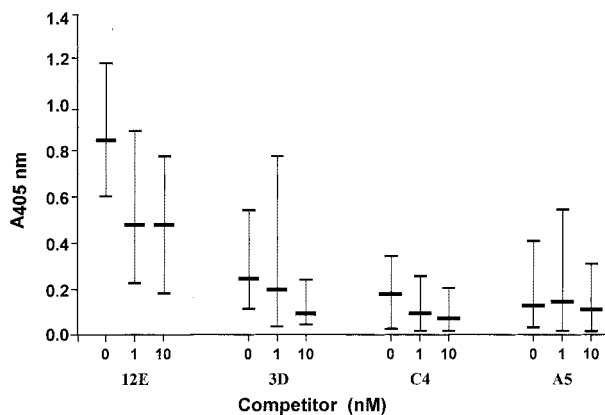


Fig. 2 Competitive ELISA. Anti-MUC-1 scFv (12E, 3D, C4, and A5) were incubated with 0, 1 or 10 nM MUC-1 competitor peptide. The results illustrate three experiments with triplicates in each experiment. The mean values and range are provided. At the 1 nM level of MUC-1 competitor peptide, the mean values were decreased most notably for the 12E, 3D, and C4 scFvs. On the addition of 10 nM of MUC-1 competitor peptide, a further decrease was observed for the 3D and C4 scFvs; no obvious further decrease in binding was observed for the 12E scFv with a 10-fold competitor increase. *P* values for the slopes extracted by covariance analysis were 0.04 for 12E, 0.04 for 3D, 0.07 for C4, and >0.1 for A5.

of the anti-MUC-1 scFvs by two different analysis methods, linear regression and covariance analysis. Results from linear regression analysis estimated the K_a for all four anti-MUC-1 scFvs tested $>1.5 \times 10^7 \text{ M}^{-1}$ (Table 1). Similar affinities were derived for the A5 ($K_a = 7.1 \times 10^8 \text{ M}^{-1}$) and C4 ($K_a = 8.2 \times 10^8 \text{ M}^{-1}$) anti-MUC-1 scFvs. Slightly lower affinities were estimated for the 3D ($K_a = 2.2 \times 10^8 \text{ M}^{-1}$) and 12E ($K_a = 1.7 \times 10^7 \text{ M}^{-1}$) scFvs. Analysis of covariance showed no significant difference in the slopes for a given scFv in the three repetitions but did show variability in the intercepts. The estimated slope for increased inhibition with increased inhibitor was statistically different from zero ($P < 0.05$) for 12E and 3D. The *P* value for C4 indicated marginal statistical significance ($P = 0.07$), and there was no significant difference for A5. Therefore, K_a s of 6.1×10^7 , 1.35×10^8 , and $6.2 \times 10^8 \text{ M}^{-1}$ were estimated for the 12E, 3D and C4 scFvs, respectively, only (Table 1).

Scatchard Analysis of the 12E scFv as ^{125}I -scFv. Because the protein shaker flask and biofermentor production was best for the 12E scFv, at ~ 1.5 to 2 mg/liter culture routinely, this scFv was chosen for additional studies. ^{125}I -anti-MUC-1 12E scFv was used to confirm the binding affinity of this molecule compared with the previous competitive ELISA assay. Two fractions purified by HPLC were analyzed: a 42 kDa fraction considered to be a naturally occurring dimeric form (divalent) of the anti-MUC-1 12E scFv, and a 25 kDa fraction representative of monomeric (monovalent) scFv form. Both forms of the anti-MUC-1 12E scFv bound the MUC-1-positive MCF-7 cells (Fig. 3). For the 12E scFv, Scatchard analysis results were also used to calculate affinity constants (K_a).

A K_a of $1.7 \times 10^8 \text{ M}^{-1}$ was determined for the purified 42 kDa fraction (dimer) of the 12E scFv, and a K_a of $8.6 \times 10^7 \text{ M}^{-1}$

Table 1 K_a s of anti-MUC-1 scFvs^a

Anti-MUC-1 scFv	Full length sequence (VH + VL)	Affinity (K_a) M^{-1}		
		Linear regression	Covariance	Scatchard
12E	Yes	1.7×10^7	6.1×10^7	1.7×10^8 (42 kDa), 8.6×10^7 (25 kDa)
A5	Yes	7.1×10^8	/	/
C4	Yes	8.2×10^8	6.2×10^8	/
3D	No VL	2.2×10^8	1.35×10^8	/

^aDetermination of the K_a s of anti-MUC-1 scFvs was based on either Scatchard analysis or competitive ELISA data. Linear regression and covariance analyses were used to extrapolate K_a s from the same competitive ELISA data. The presence or absence of VH and/or VL sequences is indicated for each scFv clone.

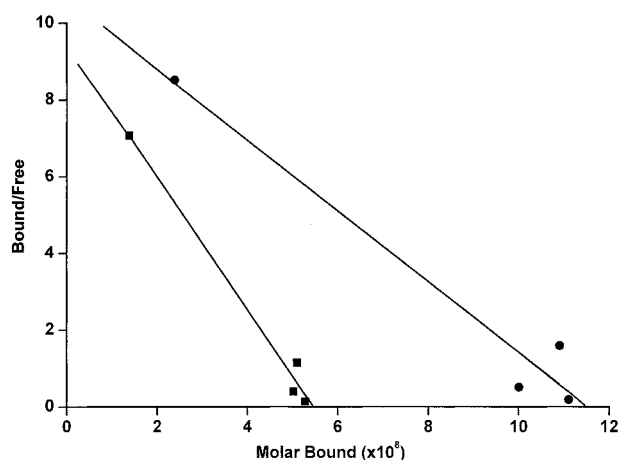


Fig. 3 Scatchard plot. Naturally occurring molecular forms of the 12E scFv (42 kDa (■) and 25 kDa (●)) were analyzed by Scatchard analysis. The 42 kDa fragment, representative of the dimeric form of 12E scFv, exhibited the greatest binding with $K_a = 1.7 \times 10^8 M^{-1}$, whereas the monomeric form of 12E exhibited $K_a = 8.6 \times 10^7 M^{-1}$.

was calculated for the purified 25 kDa fraction (monomer) of the 12E scFv (Table 1).

Molecular Model. The VH and VL antigen-binding loops are highlighted in the amino acid sequence of the 12E scFv (Fig. 4A). A three-dimensional model for the 12E scFv is provided in Fig. 4B. This model includes two structural domains corresponding to the VH and VL domains. The linker between these domains was not explicitly modeled, because the crystallographic study of the anti-CEA MFE-23 scFv (48) suggested that this linker was flexible and most likely did not assume a unique conformation. Short sequence fragments at the NH_2 and $COOH$ terminus of the 12E scFv protein, extending beyond the structure of VH and VL domains, are also expected to be flexible and were therefore not modeled. The modeled structure of the 12E scFv is very similar to that of MFE-23 scFv including four of six hypervariable antigen-binding loops. Two loops (H1 and H3) display marked differences from the MFE-23 scFv template; the H3 loop has the most dissimilar conformation.

A three-dimensional model for the 3D scFv is provided in Fig. 4C. The 3D scFv sequence includes a VH domain identical with that of the 12E scFv (Figs. 1 and 4, B and C). However, unlike that in the 12E scFv, the VL region of the 3D scFv

consisted only of short conserved NH_2 - and $COOH$ -terminal segments. Because this short composite region was flanked by a Gly/Ser-rich linker and the E-Tag that are not expected to have rigid conformations, this region is unlikely to form a stable three-dimensional structure. Secondary structure prediction for the 3D scFv protein $COOH$ -terminal sequence suggests that this composite $COOH$ -terminal region could at most, adopt a β -hairpin motif.

Immunohistochemistry. The 12E anti-MUC-1 scFv demonstrates staining of both MCF-7 cells and BT20 cells (Fig. 5, D and H). No staining of either cell line was observed using an antilymphoma control scFv (Fig. 5, C and G, 26 μ g/ml). The BrE-3 MAb, used as a positive control, demonstrated stronger staining of both cell lines, consistent with bivalent binding of a MAb compared with monovalent binding of the 12E scFv (Fig. 5, B and F). Higher concentrations of 12E demonstrated more intense staining of MCF-7 and BT20 (Fig. 5, I and J, 100 μ g/ml). No staining of the control scFv or control IgG1 was observed on breast cancer tissue (Fig. 5, K and M). MAb BrE-3 stained the breast cancer ductal carcinoma intensely (Fig. 5L). The staining pattern of breast cancer by anti-MUC-1 scFv (Fig. 5N) demonstrated similarity to staining by MAb BrE-3, consistent with the scFv targeting the breast cancer cells.

Discussion

New targeting agents are being developed for the detection and therapy of cancer. Well-characterized panels of antibody-based modules that bind cancer related antigens may provide an invaluable resource for the development of imaging, pretargeting, and therapy molecules. MUC-1 is an ideal antigen target on adenocarcinomas, because the majority of distinct MUC-1 epitopes are exposed on tumors *versus* normal tissue (21, 54). Several anti-MUC-1 scFvs were selected from an anti-MUC-1 mouse phage display library based on their ability to bind *in vitro* to a MUC-1 synthetic peptide (80 mer with 4 tandem repeats of the 20 amino acid-long tandem repeat from the extracellular domain of MUC-1) and to MCF-7 human breast cancer adenocarcinoma cell lysate. Selection of scFvs from combinatorial libraries, constructed by random assembly of VH and VL from hyperimmune lymphocyte gene pools, has the advantage of providing useful new VH and VL pairs or VH, VL unpaired units that strongly recognize antigens (55).

Sequencing of six scFvs, selected from a previously constructed mouse phage display library (42), demonstrated that four of them were full length clones (VH-linker-VL). The re-

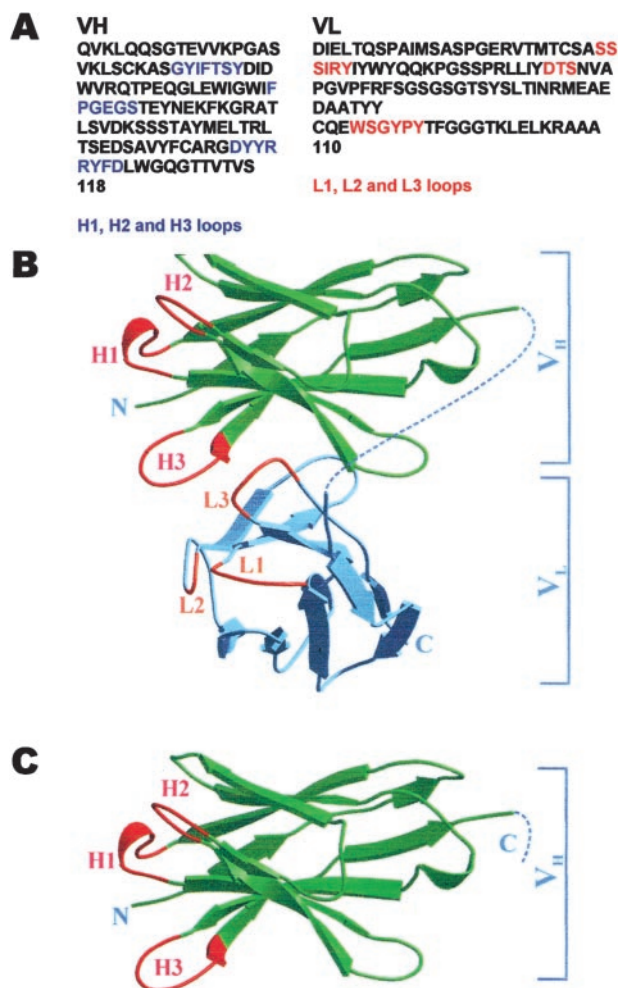


Fig. 4 Molecular models of the 12E and 3D scFvs. **A**, hypervariable antigen binding H (red) and L (blue) loops on the amino acid sequence of the VH and VL domains of the 12E scFv protein. **B**, three-dimensional structural model for the 12E scFv. VH and VL domains are green and blue, respectively. The hypervariable antigen binding loops are labeled and colored red (H1 to H3) and orange (L1 to L3). ---, approximate path of the Gly/Ser-rich linker between domains. **C**, three-dimensional structural model for the 3D (VH only) scFv.

maintaining two scFvs were partial clones coding only for either a VH or a VL region. Although unexpected, the fact that these truncated clones were selected reinforces the fact that the formation of an effective antigen-binding module from immunoglobulin genes does not necessarily require the presence of both VH and VL domains. Similar observations (56, 57), have led to the construction of a VH fusion phage library expressing VH domains only (57).

Four of the six initially selected anti-MUC-1 scFv clones were evaluated in more detail. As demonstrated by competitive ELISA, the binding of 12E, C4, and 3D (missing VL region) scFvs to MCF-7 lysate was blocked by nanomolar levels of MUC-1 competitor peptide by >40%. These observations and the initial selection by binding to synthetic MUC-1 are consistent with amino acids within the MUC-1 tandem repeats com-

prising at least part of the epitopes recognized by the selected scFvs. Linear regression analyses indicated that the four scFvs tested had K_a s in the range of 10^7 to 10^9 M^{-1} . These K_a s were confirmed by covariance analysis for all except A5. Thus, the binding affinity values of anti-MUC-1 scFvs are close to optimum for *in vivo* tumor binding, as it has been reported that affinity beyond 10^9 M^{-1} does not significantly increase tumor retention of scFvs (58). Comparisons of the K_a s obtained for the monomeric and spontaneously occurring dimeric forms of the 12E scFv by Scatchard analysis demonstrated the better binding of the dimeric form, as expected from divalent antigen binding. Antigen specificity was demonstrated by complete inhibition of radiolabeled scFv by unlabeled scFv.

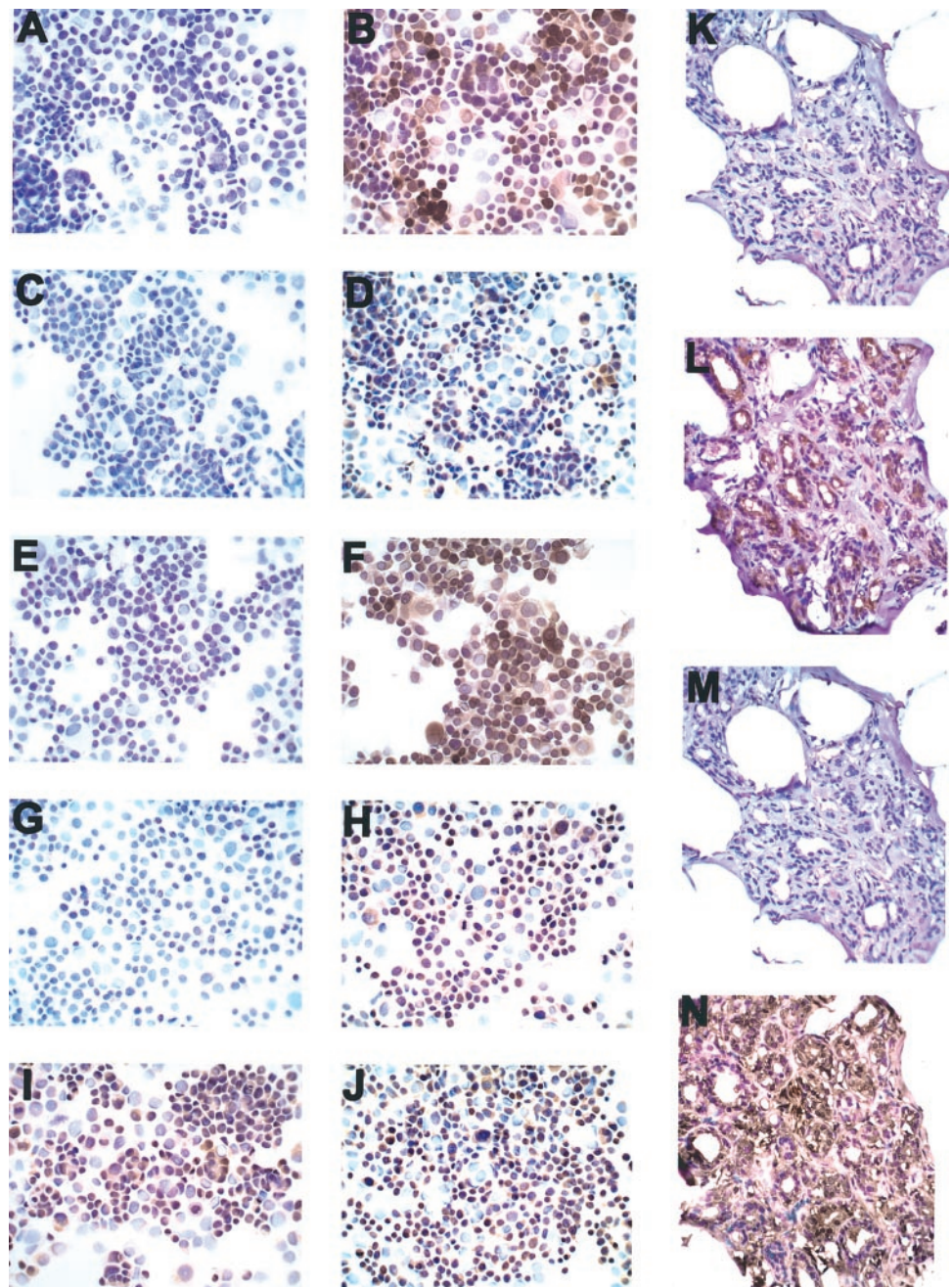
The determination of a lower binding affinity for the 12E scFv in comparison with its VH domain alone, the 3D scFv, was not anticipated. One explanation is provided by the structural molecular models established for both these proteins. As can be seen in these models, the Gly/Ser-rich linker is on the other side of the heavy chain domain hypervariable loops, making it unlikely that the COOH-terminal part of the 3D scFv would affect the interaction of these loops with the antigen. The lower antigen binding affinity determined for the 12E scFv compared with the 3D scFv could relate to decreased access to the antigen epitope by 12E because of steric hindrance caused by its VL domain. These modeled structures, combined with the binding affinity measurements, strongly suggest that in both the 12E and 3D scFv the antigen-binding was mediated by heavy chain antigen binding loops (H1 to H3). This is in good agreement with the antigen-binding model generated for MFE-23, based on the intermolecular packing in the crystal (48).

The immunohistochemistry results with scFvs from the anti-MUC-1 phage display library have shown binding to both MCF-7 and BT20 breast cancer cell lines and human breast cancer biopsy tissues. Less staining is observed on the adenocarcinoma MCF-7 cell line than on the BT20 cell line, as is also observed with the MAb BrE-3. The *in vitro* binding of anti-MUC-1 scFvs to cancer tissue as well as cancer cell lines shows promise for MUC-1 targeting cancer *in vivo*.

Studies have shown that a majority of anti-MUC-1 MABs bind tumor MUC-1 epitopes present within the highly immunogenic tandem repeats (21). Immunopathological evaluation of normal tissue suggests that most of these epitopes are inaccessible in normal tissue because of a higher degree of MUC-1 glycosylation in normal cells (59). In the case of epitopes represented on both normal and malignant tissues, their distribution on normal tissue makes the difference. Indeed, on normal tissue, MUC-1 is usually present in the luminal areas on the apical region of cells. Therefore, in therapy with blood-delivered anti-MUC-1 agents, the potentially reactive MUC-1 epitopes present on normal tissue are not being encountered. The anti-MUC-1 scFvs characterized here also recognize, at least in part, the peptidic structure of the MUC-1 antigen, which should increase their potential as candidates for tumor-specific MUC-1 binding.

ScFvs will likely be used in therapeutic applications as components of larger molecules designed to have appropriate pharmacokinetics because the scFv proteins have the physiological disadvantage of rapid elimination from the body by

Fig. 5 MAb BrE-3 and Anti-MUC-1 scFv Immunohistochemistry. *A–J*, binding of MAb BrE-3 and anti-MUC-1 scFv on MCF-7 and BT20 breast cancer cell lines. The binding of control MAb or scFv (*A, C, E, and G*) are compared with MAb BrE-3 or anti-MUC-1 scFv (*B, D, F, and H*). *A*, IgG1 on MCF-7 cells; *B*, BrE-3 on MCF-7 cells; *C*, control scFv on MCF-7 cells; *D*, anti-MUC-1 on MCF-7 cells; *E*, IgG1 on BT20 cells; *F*, BrE-3 on BT20 cells; *G*, control scFv on BT20 cells; *H*, anti-MUC-1 scFv on BT20 cells; *I*, anti-MUC-1 scFv 100 μ g/ml on MCF-7 cells; *J*, anti-MUC-1 scFv 100 μ g/ml on BT20 cells. Intense but heterogeneous binding of MAb BrE-3 is observed on both cell lines, with increased stain on BT20 cells. Less intense (heterogeneous) staining with anti-MUC-1 scFv is seen on both cell lines, with more staining observed on BT20 cells than MCF-7 cells, similar to BrE-3 staining. No staining is seen on MCF-7 or BT20 cells using either IgG1 or negative control scFv, a non-MUC-1, lymphoma-specific scFv, produced and processed (E-Tag purification) the same way as the anti-MUC-1 scFvs. *K–N*, binding of BrE-3 and anti-MUC-1 scFv on breast cancer biopsy tissue. *K*, IgG1; *L*, BrE-3; *M*, control scFv; *N*, anti-MUC-1 scFv. Cancerous ductal tissue is intensely stained by MAb BrE-3 in *L*, with similar increased stain of the cancer cells using anti-MUC-1 scFv in *N*. No staining is observed on tissue stained with IgG1 (*K*) or control scFv (*M*). Cells and tissue were photographed at $\times 400$ magnification.



the kidneys because of their small size (5, 60–64). In a pretargeted radioimmunotherapy approach, scFvs could serve as the binding elements on a molecular scaffold constructed of multispecific or bispecific agents. This would allow the small radiochelate to be administered after the pretargeting tumor binding molecule(s) localized to the tumor (65–69). The use of scFvs or subunits as components in new molecular formats offers the opportunity to assemble a tumor-seeking molecule with optimal blood and body clearance as well as tumor penetration. This study provides key information regarding the binding of scFvs to tumor antigen in the context

of molecular models, information vital to the development of new antitumor agents.

Acknowledgments

We thank Olivera Finn, Ph.D. (University of Pittsburgh School of Medicine), for generously providing the MUC-1 synthetic peptide used in these studies, and Dave Kukis, M.S., for technical assistance.

References

1. Reilly, R. M., Sandhu, J., Alvarez-Diez, T. M., Gallinger, S., Kirsh, J., and Stern, H. Problems of delivery of monoclonal antibodies. *Phar-*

- maceutical and pharmacokinetic solutions. *Clin. Pharmacokinet.*, **28**: 126–142, 1995.
2. Goldenberg, D. M. Targeted therapy of cancer with radiolabeled antibodies. *J. Nucl. Med.*, **43**: 693–713, 2002.
 3. Chang, C. H., Sharkey, R. M., Rossi, E. A., Karacay, H., McBride, W., Hansen, H. J., Chatal, J. F., Barbet, J., and Goldenberg, D. M. Molecular advances in pretargeting radioimmunotherapy with bispecific antibodies. *Mol. Cancer Ther.*, **1**: 553–563, 2002.
 4. Wu, A. M. Tools for pretargeted radioimmunotherapy. *Cancer Biother. Radiopharm.*, **16**: 103–108, 2001.
 5. Adams, G. P., McCartney, J. E., Tai, M. S., Oppermann, H., Huston, J. S., Stafford, W. F., Bookman, M. A., Fand, I., Houston, L. L., and Weiner, L. M. Highly specific *in vivo* tumour targeting by monovalent and divalent forms of 741F8 anti-*c-erbB-2* single-chain Fv. *Cancer Res.*, **53**: 4026–4034, 1993.
 6. Todorovska, A., Roovers, R. C., Dolezal, O., Kortt, A. A., Hoogenboom, H. R., and Hudson, P. J. Design and application of diabodies, triabodies and tetrabodies for cancer targeting. *J. Immunol. Methods*, **248**: 47–66, 2001.
 7. Wu, A. M., William, L. E., Zieran, L., Padma, A., Sherman, M., Bebb, G. G., Odom-Maryon, T., Wong, J. Y. C., Shively, J. E., and Raubitschek, A. A. Anti-carcinoembryonic antigen (CEA) diabody for rapid tumour targeting and imaging. *Tumor Targeting*, **4**: 1–12, 1999.
 8. Laskowski, R. A., Moss, D. S., and Thronton, J. M. Main-chain bond lengths and bond angles in protein structures. *J. Mol. Biol.*, **231**: 1049–1067, 1993.
 9. Sivolapenko, G. B., Douli, V., Pectasides, D., Skarlos, D., Sirmalis, G., Hussain, R., Cook, J., Courtenay-Luck, N. S., Merkouri, E., Konstantinides, K., and Epenetos, A. A. Breast cancer imaging with radio-labeled peptide from complementary-determining region of antitumor antibody. *Lancet*, **346**: 1662–1666, 1995.
 10. Matthey, B., Engert, A., and Barth, S. Recombinant immunotoxins for the treatment of Hodgkin's disease. *Int. J. Mol. Med.*, **6**: 509–514, 2000.
 11. Treon, S. P., Raje, N., and Anderson, K. C. Immunotherapeutic strategies for the treatment of plasma cell malignancies. *Semin. Oncol.*, **27**: 598–613, 2000.
 12. Rohrbach, F., Gerstmayer, B., Biburger, M., and Wels, W. Construction and characterization of bispecific costimulatory molecules containing a minimized CD86 (B7-2) domain and single-chain antibody fragments for tumor targeting. *Clin. Cancer Res.*, **6**: 4312–4322, 2000.
 13. Heike, Y., Kasono, K., Kunisaki, C., Hama, S., Saijo, N., Tsuruo, T., Kuntz, D. A., Rose, D. R., and Curiel, D. T. Overcoming multi-drug resistance using an intracellular MDR1 scFv. *Int. J. Cancer*, **92**: 115–122, 2001.
 14. Pavlinkova, G., Beresford, G. W., Booth, B. J. M., Batra, S. K., and Colcher, D. Pharmacokinetics and biodistribution of engineered single-chain antibody constructs of MAb CC49 in colon carcinoma xenografts. *J. Nucl. Med.*, **40**: 1536–1546, 1999.
 15. Viti, F., Tarli, L., Giovannoni, L., Zardi, L., and Neri, D. Increased binding affinity and valence of recombinant antibody fragments lead to improved targeting of tumoral angiogenesis. *Cancer Res.*, **59**: 347–352, 1999.
 16. Winter, G., Griffiths, A. D., Hawkins, R. E., and Hoogenboom, H. R. Making antibodies by phage display technology. *Annu. Rev. Immunol.*, **12**: 433–455, 1994.
 17. Clackson, T., Hoogenboom, H. R., Griffiths, A. D., and Winter, G. Making antibody fragments using phage display libraries. *Nature (Lond.)*, **352**: 624–628, 1991.
 18. Hoogenboom, H. R., de Bruine, A. P., Hufton, S. E., Hoet, R. M., Arends, J. W., and Roovers, R. C. Antibody phage display technology and its applications. *Immunotechnology*, **4**: 1–20, 1998.
 19. Phage display of peptides and proteins: a laboratory manual. San Diego: Academic Press, 1996.
 20. Barratt-Boyes, S. M. Making the most of mucin: a novel target for tumor immunotherapy. *Cancer Immunol. Immunother.*, **43**: 142–151, 1996.
 21. Price, M. R., Rye, P. D., Petrakou, E., et al. Summary report on the ISOBM TD-4 Workshop: analysis of 56 monoclonal antibodies against the MUC1 mucin. *Tumour Biol.*, **19**: 1–20, 1998.
 22. Peterson, J. A., Larocca, D., Walkup, G., Amiya, R., and Ceriani, R. L. Molecular analysis of epitopic heterogeneity of the breast mucin. In: R. L. Ceriani. (ed.), *Breast Epithelial Antigens*, pp. 55–68. New York: Plenum Publishing Corp., 1991.
 23. Gendler, S. J. MUC1, the renaissance molecule. *J. Mammary Gland Biol. Neoplasia*, **6**: 339–353, 2002.
 24. Quin, R. J., and McGucken, M. A. Phosphorylation of the cytoplasmic domain of the MUC1 mucin correlates with changes in cell-cell adhesion. *Int. J. Cancer*, **87**: 499–506, 2000.
 25. McGucken, M. A., Walsh, M. D., Hohn, B. G., Ward, B. G., and Wright, R. G. Prognostic significance of MUC1 epithelial expression in breast cancer. *Hum. Pathol.*, **26**: 432–439, 1995.
 26. Dong, Y., Walsh, M. D., Cummings, M. C., Wright, R. G., Khoo, S. K., Parsons, P. G., and McGuckin, M. A. Expression of MUC1 and MUC2 mucins in epithelial ovarian tumours. *J. Pathol.*, **183**: 311–317, 1997.
 27. Bieche, I., and Lidereau, R. A gene dosage effect is responsible for high overexpression of the *MUC1* gene observed in human breast tumors. *Cancer Genet. Cytogenet.*, **98**: 75–80, 1997.
 28. Henderson, R. A., Konitsky, W. M., Barratt-Boyes, S. M., Soares, M., Robbins, P. D., and Finn, O. J. Retroviral expression of MUC-1 human tumor antigen with intact repeat structure and capacity to elicit immunity *in vivo*. *J. Immunother.*, **21**: 247–256, 1998.
 29. Evangelou, A., Letarte, M., Marks, A., and Brown, T. J. Androgen modulation of adhesion and antiadhesion molecules in PC-3 prostate cancer cells expressing androgen receptor. *Endocrinology*, **143**: 3897–3904, 2002.
 30. Gorga, J. C., Horejsi, V., Johnson, D. R., Raghupathy, R., and Strominger, J. L. Purification and characterization of class II histocompatibility antigens from homozygous human B cell line. *J. Biol. Chem.*, **252**: 16087–16094, 1987.
 31. Pemberton, L. F., Rughetti, A., Taylor-Papadimitriou, J., and Gendler, S. J. The epithelial mucin MUC1 contains at least two discrete signals specifying membrane localization in cells. *J. Biol. Chem.*, **271**: 2332–2340, 1996.
 32. Regimbald, L. H., Pilarski, L. M., Longenecker, B. M., Reddish, M. A., Zimmermann, G., and Hugh, J. C. The breast mucin MUC1 as a novel adhesion ligand for endothelial intercellular adhesion molecule 1 in breast cancer. *Cancer Res.*, **56**: 4244–4249, 1996.
 33. Kotera, Y., Fontenot, J. D., Pecher, G., Metzgar, R. S., and Finn, O. J. Humoral immunity against a tandem repeat epitope of human mucin MUC-1 in sera from breast, pancreatic, and colon cancer patients. *Cancer Res.*, **54**: 2856–2860, 1994.
 34. Martoni, A., Zamagni, C., Bellanova, B., Zanichelli, L., Vecchi, F., Cacciari, N., Strocchi, E., and Pannuti, F. CEA, MCA, CA 15.3 and CA 549 and their combinations in expressing and monitoring metastatic breast cancer: a prospective comparative study. *Eur. J. Cancer*, **10**: 1615–1621, 1995.
 35. Richman, C. M., and DeNardo, S. J. Systemic radiotherapy in metastatic breast cancer using ⁹⁰Y-linked monoclonal MUC-1 antibodies. *Crit. Rev. Oncol. Hematol.*, **38**: 26–35, 2001.
 36. Papadimitriou, J. T., Burchell, J., Miles, D. W., and Dalziel, M. MUC-1 and cancer. *Biochim. Biophys. Acta*, **1455**: 301–313, 1999.
 37. Maraveyas, A., Snook, D., Hird, V., Kosmas, C., Meares, C. F., Lambert, H. E., and Epenetos, A. A. Pharmacokinetics and toxicity of an yttrium-90-CITC-DTPA-HMFG1 radioimmunoconjugate for intraperitoneal radioimmunotherapy of ovarian cancer. *Cancer (Phila.)*, **73**: 1067–1075, 1994.
 38. DeNardo, S. J., Kramer, E. L., O'Donnell, R. T., Richman, C. M., Salako, Q. A., Shen, S., Noz, M., Glenn, S. D., Ceriani, R. L., and DeNardo, G. L. Radioimmunotherapy for breast cancer using indium-111/yttrium-90 BrE-3: results of a phase I clinical trial. *J. Nucl. Med.*, **38**: 1180–1185, 1997.

39. Kramer, E. L., Liebes, L., Wasserheit, C., Noz, M. E., Blank, E. W., Zabalegui, A., Melamed, J., Furmanski, P., Peterson, J. A., and Ceriani, R. L. Initial clinical evaluation of radiolabeled MX-DTPA humanized BrE-3 antibody in patients with advanced breast cancer. *Clin. Cancer Res.*, *4*: 1679–1688, 1998.
40. Schrier, D. M., Stemmer, S. M., Johnson, T., Kasliwal, R., Lear, J., Matthes, S., Taffs, S., Dufton, C., Glenn, S. D., Butchko, G., Ceriani, R. L., Rovira, D., Bunn, P., Shpall, E. J., Bearman, S. I., Purdy, M., Cagnoni, P., and Jones, R. B. High-dose ⁹⁰Y Mx-diethylenetriamine-pentaacetic acid (DTPA)-BrE-3 and autologous hematopoietic stem cell support (AHSCS) for the treatment of advanced breast cancer: a phase I trial. *Cancer Res.* *55*: 5921s–5924s, 1995.
41. Cagnoni, P. J., Ceriani, R. L., Cole, W. C., et al. Phase I study of high-dose radioimmunotherapy with 90-Y-hu-BrE-3 followed by autologous stem cell support (ASCS) in patients with metastatic breast cancer. *Cancer Biother. Radiopharm.*, *13*: 328, 1998.
42. Winthrop, M. D., DeNardo, S. J., and DeNardo, G. L. Development of a hyperimmune anti-MUC-1 single chain antibody phage display library for targeting breast cancer. *Clin. Cancer Res.*, *10*: 3088–3094, 1999.
43. Gendler, S., Taylor-Papadimitriou, J., Duhig, T., Rothbard, J., and Burchell, J. A highly immunogenic region of a human polymorphic epithelial mucin expressed by carcinomas is made up of tandem repeats. *J. Biol. Chem.*, *263*: 12820–12823, 1988.
44. Sambrook J. *Molecular Cloning: a Laboratory Manual*. NY: Cold Spring Harbor, 1989.
45. Goshorn, S., Sanderson, J., Axworthy, D., Lin, Y., Hylarides, M., and Schultz, J. Preclinical evaluation of a humanized NR-LU-10 antibody-streptavidin fusion protein for pretargeted cancer therapy. *Cancer Biother. Radiopharm.*, *16*: 109–123, 2001.
46. Fontenot, J. D., Tjandra, N., Bu, D., Ho, C., Montelaro, R. C., and Finn, O. J. Biophysical characterization of one-, two-, and three-tandem repeats of human mucin (MUC-1) protein core. *Cancer Res.*, *53*: 5386–5394, 1993.
47. Schier, R., Marks, J. D., Wolf, E. J., Apell, G., Huston, J. S., Weiner, L. M., and Adams, G. P. *In vitro* and *in vivo* characterization of a human anti-c-erbB-2 single chain Fv isolated from a filamentous phage antibody library. *Immunotechnology*, *1*: 63–71, 1995.
48. Boehm, M. K., Corper, A. L., Wan, T., Sohi, M. K., Sutton, B. J., Thronton, J. D., Keep, P. A., Chester, K. A., Begent, R. H., and Perkins, S. J. Crystal structure of the anti-(carcinoembryonic antigen) single-chain Fv antibody MFE-23 and for antigen binding based on intermolecular contacts. *Biochem. J.*, *346*: 519–528, 2000.
49. Jones, D. T. Protein secondary structure prediction based on position-specific scoring matrices. *J. Mol. Biol.*, *292*: 195–202, 1999.
50. Sali, A., and Blundell, T. L. Comparative protein modelling by satisfaction of spatial restraints. *J. Mol. Biol.*, *234*: 779–815, 1993.
51. Blank, E. W., Pant, K. D., Chan, C. M., Peterson, J. A., and Ceriani, R. L. A novel anti-breast epithelial mucin MoAb (BrE-3). *Cancer (Phila.)*, *5*: 38–44, 1992.
52. Howell, L. P., DeNardo, S. J., Levy, N., Lund, J., and DeNardo, G. L. Immunohistochemical staining of metastatic ductal carcinomas of the breast by monoclonal antibodies used in imaging and therapy: a comparative study. *Int J Biol Markers*, *10*: 126–135, 1995.
53. DeNardo, D. G., Xiong, C. Y., Shi, X. B., DeNardo, G. L., and DeNardo, S. J. Anti-HLA-DR/anti-DOTA diabody construction in a modular gene design platform: bispecific antibodies for pretargeted radioimmunotherapy. *Cancer Biother. Radiopharm.*, *16*: 525–535, 2001.
54. Sikut, R., Sikut, A., Zhang, K., Baeckstrom, D., and Hansson, G. C. Reactivity of antibodies with highly glycosylated MUC1 mucins from colon carcinoma cells and biles. *Tumour Biol.*, *19*: 122–126, 1998.
55. Marks, C., and Marks, J. D. Phage libraries: a new route to clinically useful antibodies. *N. Engl. J. Med.*, *335*: 730–733, 1996.
56. Mulydermans, S., and Lauwereys, M. Unique single-domain antigen binding fragments derived from naturally occurring camel heavy chain antibodies. *J. Mol. Recognit.*, *12*: 131–140, 1999.
57. Cai, X., and Garen, A. Comparison of fusion phage libraries displaying VH or single-chain Fv antibody fragments derived from the antibody repertoire vaccinated melanoma patient as a source of melanoma-specific targeting molecules. *Proc. Natl. Acad. Sci. USA*, *94*: 9261–9262, 1997.
58. Adams, G. P., Schier, R., McCall, A. M., Simmons, H. H., Horak, E. M., Alpaugh, R. K., Marks, J. D., and Weiner, L. M. High affinity restricts the localization and tumor penetration of single-chain Fv antibody molecules. *Cancer Res.*, *61*: 4750–4755, 2001.
59. Ho, S. B., Niehans, G. A., Lyftogt, C., Yan, P. S., Cherwitz, D. L., Gum, E. T., Dahiya, R., and Kim, Y. S. Heterogeneity of mucin gene expression in normal and neoplastic tissues. *Cancer Res.*, *53*: 641–651, 1993.
60. Wu, A. M., Chen, W., Raubitschek, A., Williams, L. E., Neumaier, M., Fischer, R., Hu, S. Z., Odom-Maryon, T., Wong, J. Y., and Shively, J. E. Tumor localization of anti-CEA single-chain Fvs: improved targeting by non-covalent dimers. *Immunotechnology*, *2*: 21–36, 1996.
61. Dall'Acqua, W., and Carter, P. Antibody engineering. *Curr. Opin. Struct. Biol.*, *8*: 443–450, 1998.
62. Adams, G. P. Improving the tumor specificity and retention of antibody-based molecules. *In Vivo*, *12*: 11–22, 1998.
63. Begent, R. H. J., Verhaar, M. J., Chester, K. A., Casey, J. L., Green, A. J., Napier, M. P., Hope-Stone, L. D., Cushen, N., Keep, P. A., Johnson, C. J., Hawkins, R. E., Hilsen, A. J. W., and Robson, L. Clinical evidence of efficient tumor targeting based on single-chain Fv antibody selected from a combinatorial library. *Nat. Med.*, *2*: 979–984, 1996.
64. DeNardo, S. J., DeNardo, G. L., DeNardo, D. G., Xiong, C. Y., Shi, X. B., Winthrop, M. D., Kroger, L. A., and Carter, P. Antibody phage libraries for the next generation of tumor targeting radioimmunotherapeutics. *Clin. Cancer Res.*, *10*: 3213–3218, 1999.
65. Goodwin, D. A. Tumor pretargeting: almost the bottom line. *J. Nucl. Med.*, *36*: 876–879, 1995.
66. Chinol, M., Paganelli, G., Sudati, F., Meares, C., and Fazio, F. Biodistribution in tumour-bearing mice of two Y-90-labelled biotins using three-step tumour targeting. *Nucl. Med. Commun.*, *18*: 176–182, 1997.
67. van Osdol, W. W., Sung, C., Dedrick, R. L., and Weinstein, J. N. A distributed pharmacokinetic model of two-step imaging and treatment protocols: application to streptavidin-conjugated monoclonal antibodies and radiolabeled biotin. *J. Nucl. Med.*, *34*: 1552–1564, 1993.
68. Hnatowich, D. J., Virzi, F., and Doherty, P. W. DTPA-coupled antibodies labeled with yttrium-90. *J. Nucl. Med.*, *26*: 503–509, 1985.
69. Cremonesi, M., Ferrari, M., Chinol, M., Stabin, M. G., Grana, C., Prisco, G., Robertson, C., Tosi, G., and Paganelli, G. Three-step radioimmunotherapy with yttrium-90 biotin: dosimetry and pharmacokinetics in cancer patients. *Eur. J. Nucl. Med.*, *26*: 110–120, 1999.